The Journal of Experimental Biology 214, 1546-1553
© 2011. Published by The Company of Biologists Ltd
doi:10.1242/jeb.037804

RESEARCH ARTICLE

Whole-body kinematics of a fruit bat reveal the influence of wing inertia on body accelerations

José Iriarte-Díaz[1,2,*], Daniel K. Riskin[1,†], David J. Willis[3], Kenneth S. Breuer[4] and Sharon M. Swartz[1,4]

[1]Department of Ecology and Evolutionary Biology, Brown University, Providence, RI 02912, USA, [2]Department of Organismal Biology and Anatomy, University of Chicago, Chicago, IL 60637, USA, [3]Department of Mechanical Engineering, University of Massachusetts, Lowell, MA 01854, USA and [4]Division of Engineering, Brown University, Providence, RI 02912, USA

*Author for correspondence (jiriarte@uchicago.edu)

[†]Present address: Department of Biology, City College of the City University of New York, New York, NY 10031, USA

Accepted 25 January 2011

SUMMARY

The center of mass (COM) of a flying animal accelerates through space because of aerodynamic and gravitational forces. For vertebrates, changes in the position of a landmark on the body have been widely used to estimate net aerodynamic forces. The flapping of relatively massive wings, however, might induce inertial forces that cause markers on the body to move independently of the COM, thus making them unreliable indicators of aerodynamic force. We used high-speed three-dimensional kinematics from wind tunnel flights of four lesser dog-faced fruit bats, *Cynopterus brachyotis*, at speeds ranging from 2.4 to 7.8 m s^{-1} to construct a time-varying model of the mass distribution of the bats and to estimate changes in the position of their COM through time. We compared accelerations calculated by markers on the trunk with accelerations calculated from the estimated COM and we found significant inertial effects on both horizontal and vertical accelerations. We discuss the effect of these inertial accelerations on the long-held idea that, during slow flights, bats accelerate their COM forward during 'tip-reversal upstrokes', whereby the distal portion of the wing moves upward and backward with respect to still air. This idea has been supported by the observation that markers placed on the body accelerate forward during tip-reversal upstrokes. As in previously published studies, we observed that markers on the trunk accelerated forward during the tip-reversal upstrokes. When removing inertial effects, however, we found that the COM accelerated forward primarily during the downstroke. These results highlight the crucial importance of the incorporation of inertial effects of wing motion in the analysis of flapping flight.

Supplementary material available online at http://jeb.biologists.org/cgi/content/full/214/9/1546/DC1

Key words: flight, inertia, kinematics, upstroke, bat, center of mass.

INTRODUCTION

The flapping flight of animals is complex, and many basic questions about how bats, birds and insects fly have yet to be answered. Bats modulate their wing kinematics in subtle but predictable ways to fly at different speeds (Aldridge, 1986; Aldridge, 1987; Lindhe Norberg and Winter, 2006; Norberg, 1976; Riskin et al., 2008; Wolf et al., 2010), but the precise mechanisms by which aerodynamic forces are modulated to control forward velocity and effect maneuvers remain poorly understood. To accelerate during forward flight, any flying organism must produce a net aerodynamic force to counteract gravity and overcome drag (Fig. 1A). This force can be decomposed into a net force component in the direction of flight that corresponds to the difference between thrust and drag, i.e. net thrust, and a perpendicular component that corresponds to the difference between lift and weight (Fig. 1A). During forward, steady flight, the average lift over the course of a wingbeat must equal body weight, and average thrust must equal drag. However, unlike airplanes, flying organisms cannot continuously generate constant lift and thrust because of the oscillatory nature of flapping, so instantaneous force generation varies across the wingbeat cycle. As a consequence, a flying bat will accelerate and decelerate throughout a wingbeat, even during steady-state flights where average acceleration is zero over the complete cycle. The timing of the instantaneous net force generation in the wingbeat cycle is the focus of this study.

Studying the dynamics of organisms moving in a fluid is not a simple task. One method that has been used to estimate net aerodynamic forces during flight is to record the instantaneous position of markers fixed on the trunk of a flying organism, under the assumption that the computed accelerations of these trunk markers accurately reflect the accelerations of the center of mass (COM) of the organism (e.g. Thomas et al., 1990). However, it is possible that the location of a bat's COM relative to the trunk can vary considerably over the wingbeat cycle. This possibility arises because bats possess relatively massive wings, and changes in mass distribution will occur when the wings move relative to the body, which can be interpreted as the trunk being moved around the COM by inertial forces produced by the flapping motions of the wings (Fig. 1B). As a result, accelerations computed from the position of landmarks placed on the trunk will not necessarily represent accelerations of the bat's COM. Instead, accelerations computed from landmarks on the trunk result from gravitational and aerodynamic forces acting on the COM in addition to inertial forces, produced by the motion of the wings, acting on the body. Inertial forces are likely to be significant in bats because the mass of the wings comprises a significant portion of total body mass, ranging

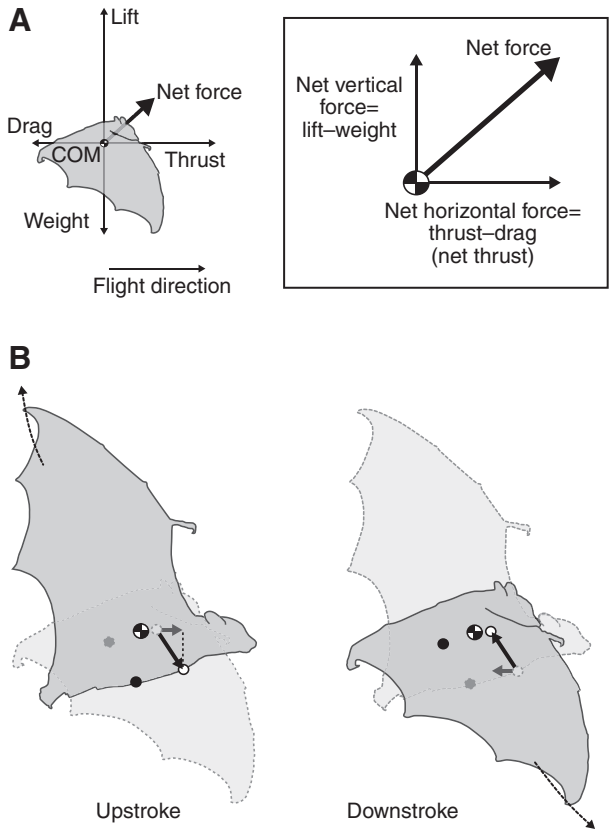

Fig. 1. (A) Free-body diagram of a bat in accelerating flight, indicating the aerodynamic and gravitational forces that accelerate the center of mass (COM). Lift is perpendicular to the direction of flight whereas drag and thrust are parallel to the direction of flight. The net force produced can be decomposed into net force components parallel and perpendicular to the direction of flight (see inset). The parallel component corresponds to the net thrust. Thus, measurements of the acceleration of the COM would directly reflect the net forces acting on it. (B) Effect of the oscillation of the wings on the position of the COM and accelerations of the body. When external forces, such as aerodynamic and gravitational forces, are absent, the position of the COM will remain constant but the body moves in opposition to the flapping wings to conserve momentum. Closed and open symbols correspond to the pelvis and chest markers, respectively. During upstroke, the upward and backward acceleration of the wings will produce an inertial force (black arrow) that will move the body forward and downward with respect to the downstroke. This force will produce a forward-oriented component, or inertial thrust, during upstroke (grey arrow). During downstroke (solid bat), the downward and forward acceleration of the wings will produce an inertial force (black arrow) that will move the body backward and upward while keeping the position of the COM constant. The horizontal component of this inertial force will produce negative inertial thrust during downstroke (grey arrow).

from 11 to 20% (Thollesson and Norberg, 1991; Watts et al., 2001), and because bats' wings undergo large accelerations. Indeed, in birds with relative wing mass comparable to that of bats, inertial forces have been estimated to contribute a significant proportion of the total body accelerations, e.g. 25–33% in pigeons (Bilo et al., 1984) and 50% in cockatiels (Hedrick et al., 2004). If the motions of the wings in bats are as great or greater than those of pigeons or cockatiels, inertial forces are also likely to be substantial; therefore, those forces should be estimated in studies of bat flight.

In the present study, we evaluated the effect of inertial forces produced by the motion of the wings on the estimation of net instantaneous aerodynamic forces during flight in bats by employing a detailed model of the mass distribution of the bat's body and wings throughout the wingbeat cycle. By applying an inertial analysis, we hope to obtain new insight into the relative importance of different parts of the wingbeat cycle to net aerodynamic force production. Specifically, we focus on the long-held idea that the upstroke portion of the wingbeat cycle is an important if not the main generator of forward net acceleration for slow-flying bats.

In slow flight, several species of bats and birds use a distinctive characteristic 'tip-reversal' or 'back-flick' upstroke, in which the distal portion of the wing is moved upwards and backwards with respect to still air (Aldridge, 1986; Aldridge, 1987; Alexander, 2002; Azuma, 2006; Brown, 1948; Norberg, 1976; Norberg, 1990; Tobalske, 2007; Wolf et al., 2010). These tip-reversals are believed to generate an aerodynamic force in the direction of flight, i.e. thrust, during the upstroke (Aldridge, 1987; Brown, 1953; Lindhe Norberg and Winter, 2006; Norberg, 1976; Norberg, 1990). Two mechanisms have been proposed by which tip-reversal upstrokes in bats should result in thrust during the upstroke portion of the wingbeat cycle (Aldridge, 1991). First, the ventral surface of the handwing faces forward and upward, with a positive angle of attack, during some portion of the upstroke, resulting in vertical support and forward-directed force during that portion of the stroke. Second, the backward motion of the handwing with respect to still air, even with negative angles of attack, could produce considerable drag, resulting in a forward-directed force component (i.e. thrust).

On average, thrust produced throughout the wingbeat cycle must equal drag during steady flight. It has been argued that, in some cases, most of the thrust required during slow, steady flight is generated during the upstroke portion of the wingbeat cycle. For example, a classic study of the kinematics of *Plecotus auritus* in forward flight at $2.3\,m\,s^{-1}$ estimated the coefficients of lift and drag of the wings using steady-state aerodynamic theory, predicting that most of the required thrust is provided during upstroke whereas weight support was produced during downstroke (Norberg, 1976). Recent experimental evidence using particle image velocimetry (PIV) has shown thrust generation during upstroke in one bat species during slow flight (Hedenström et al., 2007; Johansson et al., 2008). However, without estimating the drag component it is difficult to assess the relative contribution of the phases of the wingbeat cycle to forward acceleration. For example, generation of thrust during upstroke could be coupled with an increase in drag and, therefore, the net effect on the COM could be a reduced or even negative forward acceleration. Unfortunately, because of the nature of thrust and drag, estimation of drag remains technically difficult (Barlow et al., 1999; Hedenström et al., 2009); therefore, the relative importance of the upstroke portion of the wingbeat cycle in producing forward acceleration of the COM during flight is still unclear. Thus, we focus our study on the net vertical and horizontal accelerations generated during the upstroke and downstroke phases of the wingbeat cycle, and we discuss the implications of the inertial effects produced by the movement of the wings on the hypothesis that wingtip reversal in slow flight generates a net forward force during the upstroke.

MATERIALS AND METHODS

Animals and experimental procedures

Four female lesser dog-faced fruit bats, *Cynopterus brachyotis* (Müller 1838), on loan from the Lubee Bat Conservancy (Gainesville, FL, USA), were the subjects of this experiment (Table 1). They were housed in the animal care facilities of the Harvard University Concord Field Station (Bedford, MA, USA), where they were provided with food and water *ad libitum*. Bats

Table 1. Morphological measurements of the *Cynopterus brachyotis* individuals used in this study

Variable	Bat 1	Bat 2	Bat 3	Bat 4
Mass (kg)	0.0348	0.0371	0.0417	0.0331
Wing span (m)	0.361	0.386	0.411	0.355
Wing area (m^2)	0.0197	0.0212	0.0250	0.0188
Aspect ratio	6.6	7.0	6.8	6.7
Wing loading (N m^{-2})	17.3	17.2	16.3	17.3

were anesthetized with isoflurane gas prior to each experimental session and key anatomical landmarks were marked with high-contrast, non-toxic white paint on the undersurface of one wing and on the trunk (Fig. 2A). Bats were trained to fly at the center of the wind tunnel chamber over a range of air speeds from 2.4 to 7.8 m s^{-1}. For each individual, a minimum of six different speeds were recorded. The Concord Field Station wind tunnel is an open-circuit tunnel with a closed test section in the flight chamber and a working section of 1.4×1.2×1.2 m length×width×height (Fig. 2B). Technical details and aerodynamic characteristics of the wind tunnel were described by Hedrick et al. (Hedrick et al., 2002).

All components of this study were approved by the Institutional Animal Care and Use Committees at Brown University, Harvard University and the Lubee Bat Conservancy, and by the Division of Biomedical Research and Regulatory Compliance of the Office of the Surgeon General, United States Air Force.

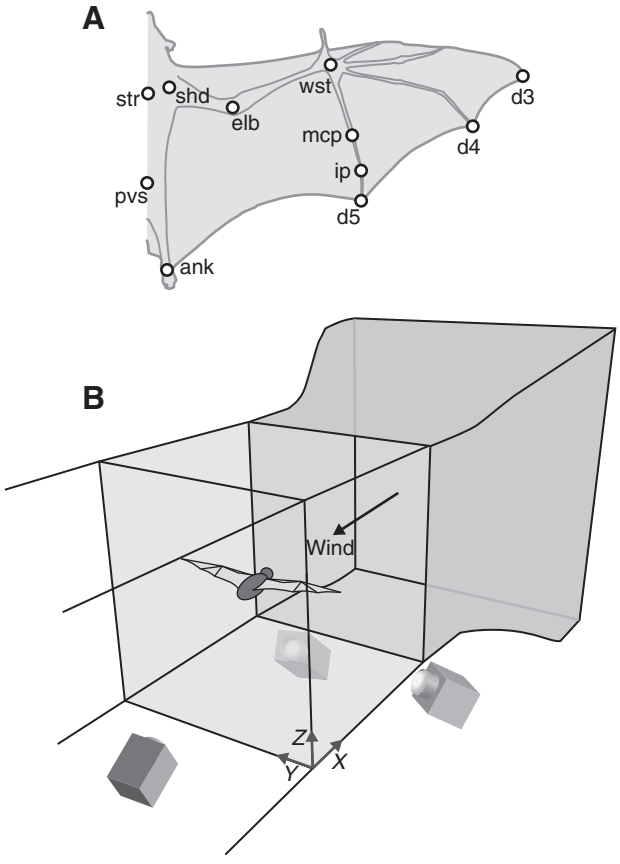

Fig. 2. Schematic diagram of (A) the ventral view of a bat indicating the position of the body and wing markers used to calculate kinematic parameters and (B) the experimental setup of the wind tunnel. Three high-speed digital cameras were positioned outside of the working section of the wind tunnel as shown. Not to scale. ank, ankle; d3, d4 and d5, distal end of of distal phalanx of digits III, IV and V, respectively; ip, interphalangeal joint of digit V; mcp, metacarpal-phalangeal joint of digit V; pvs, pelvis; shd, shoulder; str, sternum; wst, wrist.

Three-dimensional coordinate mapping

Flights were recorded at 1000 frames s^{-1} with 1024×1024 pixel resolution using three phase-locked high-speed Photron 1024 PCI digital cameras (Photron USA, Inc., San Diego, CA, USA). The volume of the wind tunnel in which the bat was flown was calibrated using the direct linear transformation (DLT) method, based on a 40-point calibration cube (035×0.35×0.29 m) recorded at the beginning of each set of trials (Abdel-Aziz and Karara, 1971). From each video frame, 11 anatomical markers were digitized (Fig. 2A) using DLTdv3 software for MATLAB (Hedrick, 2008). The three-dimensional position of each marker was resolved by the DLT coefficients obtained from the calibration cube (Abdel-Aziz and Karara, 1971). Gaps in the three-dimensional data occurred when a marker was not visible in at least two cameras. These were filled by interpolation, using an over-constrained polynomial fitting algorithm (Riskin et al., 2008). For single gaps of up to six frames with at least six digitized points at either side of the gap, a third-order over-constrained polynomial fit was used. For gaps that included sporadic intermediate points, a sixth-order polynomial was used. After gap filling, a 50 Hz digital Butterworth low-pass filter was used to remove high-frequency noise. This cut-off frequency was approximately 5 to 6 times higher than the wingbeat frequency recorded in our bats.

Determination of kinematic parameters

Wingbeat kinematics were obtained for each speed; we recorded a flight from each bat at each speed, then constructed a mean value of all wingbeat cycles (three to seven wingbeats) for each individual for each speed. We defined downstroke and upstroke phases of the wingbeat cycle by the downward *versus* upward movement of the wrist marker relative to the body, and accelerations were calculated for the downstroke and upstroke separately. The phases of the wingbeat cycle defined by the wrist are usually offset to the phases defined by the motion of the wingtip, which is sometimes used to define the phases of the wingbeat cycle for bats, birds or insects. We prefer to employ the motion of the wrist to define wingbeat phase in bats because it appears to be under more direct neuromuscular control, with the somewhat delayed movements of the handwing following, in part, by passive motion. The beginning of the downstroke defined by the wrist preceded that of the wingtip by *ca.* 8 ms, 6% of the wingbeat period, and the downstroke of the wrist preceded that of the wingtip by *ca.* 12 ms, 9% of the wingbeat period. Thus, mean accelerations during both downstroke and upstroke may vary depending on the definition of phases of the wingbeat cycle. On average, the variations arising from the definition of wingbeat phase were small: horizontal accelerations differed by 4–11% and vertical accelerations by 3–9%. These differences, in the case of this particular study, have only minor quantitative and qualitative effects upon the results of the analyses presented.

Only trials where the magnitude of the mean acceleration over a wingbeat cycle was less than 1.5 m s^{-2} were used. Two trials (both at high speeds) were removed from the analysis because net vertical accelerations exceeded this value. For vertical and horizontal accelerations, more than 75% of the data were within the range between –0.9 and 0.9 m s^{-2}. The flight speeds we report correspond to airspeed with respect to the bat's body, calculated as the bat's speed with respect to the wind tunnel plus the wind speed inside the chamber. Wingbeat frequency was calculated as the inverse of

the period between the beginnings of two consecutive downstrokes. Wingbeat amplitude was calculated as the three-dimensional angle between the line connecting the wingtip and shoulder markers at the beginning of the downstroke, and the line connecting the wingtip and shoulder markers at the end of the downstroke. Stroke plane angle was calculated as the angle between the horizontal axis and the least-squares regression line through the lateral projection of the wingtip position during the downstroke (Riskin et al., 2010).

Accelerations were calculated as follows:

(1) Accelerations of the trunk were estimated by independently computing the accelerations of the sternum and pelvis markers as the second derivatives of each of the markers' positions over time. These accelerations correspond to accelerations produced by gravity and aerodynamic forces acting on the COM in addition to inertial forces generated by the motion of the wings acting on the body.

(2) Aerodynamic accelerations of the COM were computed by estimating the location of the COM at each time step, using the mass model described below. The second derivative of the estimated COM position with respect to time corresponds to the accelerations produced by both aerodynamic forces and gravity.

(3) Inertial accelerations produced by the motion of the wings were calculated as the difference between accelerations of the trunk and aerodynamic accelerations of the COM.

Using this method, instantaneous horizontal accelerations of the COM in the direction of flight represent net thrust, i.e. the imbalance between thrust produced by the wings and the drag produced by the whole body (Fig. 1A). Because drag is present throughout the wingbeat cycle, zero acceleration of the COM in the direction of flight indicates that thrust equals drag, i.e. there is no net thrust.

Mass model

The mass model of dynamic change in location of the COM is a time-varying discrete approximation of the bat's mass distribution, based on the location of the markers. To develop the discrete mass system representing the bat, we partitioned total body mass into individual components or regions. The wing membrane, wing bones and trunk were treated as separate objects, each with its own mass and time-dependent position, which were combined to form the total mass model.

To model the distribution of the wing-membrane mass, we constructed a triangulation of the wing geometry at each time step. The large-scale base triangulation was developed using the location of the marker positions at a given time, and a subsequent subdivision of those triangles was performed to give a mesh of fine-scale triangular elements (Fig. 3A). Each triangular element of the membrane, T_i, was assigned a constant thickness (1×10^{-4} m) and density (1×10^{3} kg m^{-3}) based on measured characteristics of bat wing-membrane skin (Swartz et al., 1996). A resulting discrete point mass, m_i, for each triangular membrane element was computed based on the volume of that triangular membrane and assigned a position at the centroid of the triangle element.

To model the distribution of mass among and within each of the wing bones, we constructed a curve connecting the markers located at the endpoints of the bones. Digits I (thumb) and II were not considered in this model. Because of the small size of the thumb with respect to the overall wing, it is expected to have a small effect on the results of the model. The second digit, however, might have a slightly larger effect. In both instances, excluding the digits from the model led to the expectation that our model slightly underestimates the inertial effect of the wing motion. The curve for each bone in the wing was defined from the location of the markers. Given the tapered shape of bat bones (Swartz, 1997), the

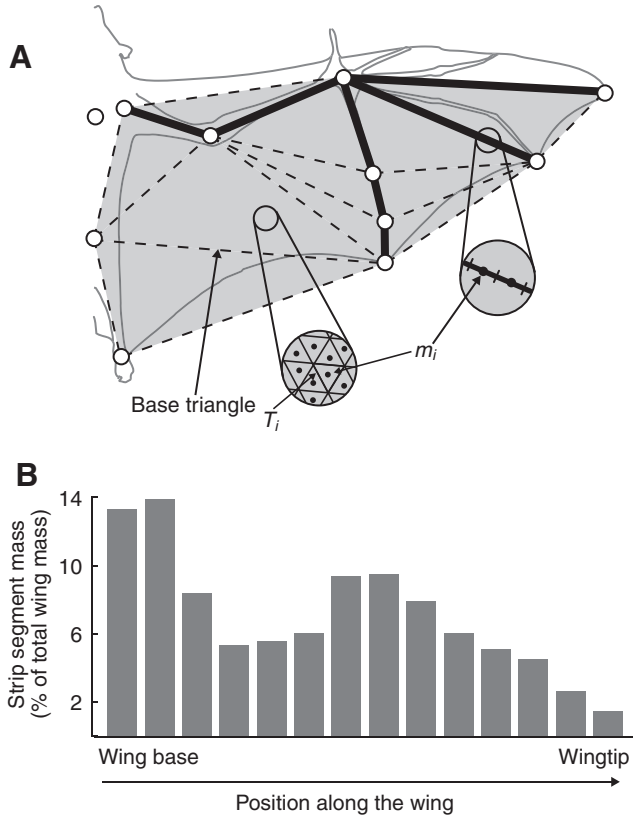

Fig. 3. (A) Schematic diagram of the mass distribution model used to calculate the COM of the bat. The thick lines represent the wing bones, each of which is assigned a given mass based on dimensions and bone density. The triangular patches represent the base triangles of the skin mass model, and insets show detailed subdivisions of bone and skin masses (m_i) and individual triangular elements (T_i) of the model. (B) Representative mass distribution along the wing as a percentage of the total wing mass during mid-downstroke of *Cynopterus brachyotis* flying at 2.9 m s^{-1}.

cross-sectional radius of each bone element of the model was defined by a quadratic function with respect to the length of the bone. We assigned a constant density to the bones (2×10^{3} kg m^{-3}) based on typical values for compact cortical bone in mammals. Using the distribution of bone radii and the location of the bone elements in space, the line was subdivided into smaller line elements, from which discrete mass points were defined. The mass of the wings was scaled such that the constructed distribution comprises 16% of total body mass, a conservative estimate, consistent with patterns in bats of similar size (Thollesson and Norberg, 1991). The mass and moment of inertia of the wing with respect to the shoulder (Fig. 3B) was compared with measured values (Thollesson and Norberg, 1991) to ensure that the model was physically realistic. Finally, the bat's thorax plus abdomen was defined as a three-dimensional ellipsoid.

The element-wise discrete mass representation of the membranes, bones and body, m_i, was combined with detailed kinematic records of motion of each landmark to determine the overall location of the bat COM ($\mathbf{r}_{COM}$), using the equation:

$$\mathbf{r}_{COM} = \frac{\sum \mathbf{r}_i\, m_i}{m_T}\ , \qquad (1)$$

where $\mathbf{r}_i$ is the position vector of the ith discrete point mass and m_T is the total mass of the bat.

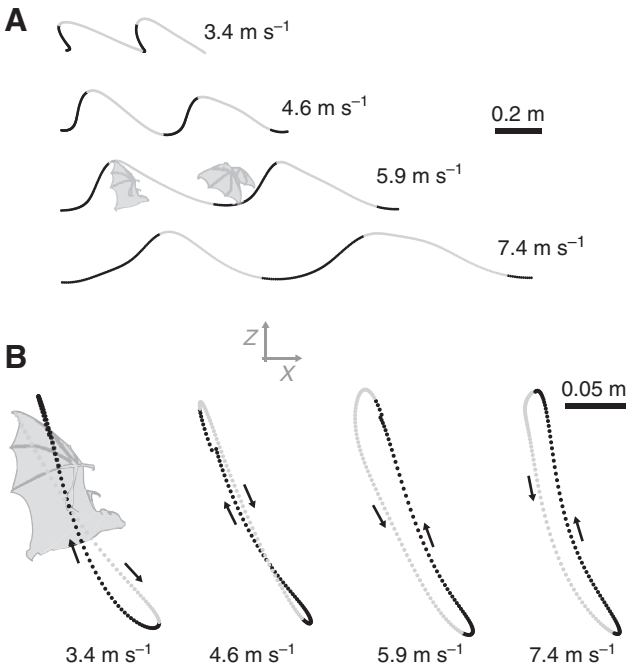

Fig. 4. Lateral projection of the trace of the wingtip over two wingbeats for a bat flying at different speeds, with respect to still air (A) and with respect to its own body (B). Grey traces correspond to the downstroke portion of the wingbeat. Note in A that, at the slowest speed depicted (3.4 m s^{-1}), the wingtip moves posteriorly during part of the upstroke, but this pattern diminishes with increases in speed.

Statistical analyses

Statistical analyses were conducted using JMP 6 (SAS Institute, Cary, NC, USA) and MATLAB R2008a (The MathWorks, Natick, MA, USA). Regression analyses were performed with general linear models (GLMs) with individuals as a factor and flight speed as a covariate. Slopes among individuals were not significantly different unless specifically indicated. Values are reported as means ± s.e.m.

RESULTS

Bats flew in the wind tunnel at speeds ranging from 2.4 to 7.8 m s^{-1}, with wingbeat frequencies ranging between 7.6 and 9.9 Hz, wingbeat amplitudes from 50 deg during slow flights to 140 deg during fast flights, and stroke plane angles from 40 deg during slow flight to 80 deg during fast flight (see supplementary material Fig. S1). The path of the wingtip with respect to still air showed that bats flying at low speeds moved their wings upward and backward during upstroke, producing a tip-reversal at speeds below 3.7 m s^{-1} (Fig. 4A). This back-flick was observed only at the distal portion of the handwing; in three cases, all at speeds below 2.6 m s^{-1}, the wrist also produced a back-flick. As speed increased, the backward movement of the wingtip gradually disappeared, becoming an upward and forward motion of the wingtip (Fig. 4A). The horizontal excursion of the wingtip with respect to the body decreased as speed increased (GLM, speed effect: slope=–0.015, $F_{1,17}$=39.4, P<0.0001) whereas vertical excursion increased with speed (GLM, speed effect: slope=0.014, $F_{1,17}$=19.5, P<0.001). As a result, stroke plane angle became more vertical as speed increased.

Horizontal and vertical accelerations of the COM and of markers on both the sternum and the pelvis changed cyclically throughout the wingbeat cycle, but the phases of their oscillations were offset. At slow speeds, body markers decelerated in the forward flight direction during most of the downstroke and then accelerated during the end of the downstroke and most of the upstroke (Fig. 5A). As flight speed increased, forward body acceleration reached a maximum earlier in the wingbeat cycle, around the downstroke–upstroke transition (Fig. 5B). In contrast, the COM accelerated forward during downstroke and decelerated during mid-upstroke and part of the downstroke during both slow and fast flight (Fig. 5). In some cases, we observed a decrease in the change of acceleration of the COM during mid-upstroke during slow flight, suggesting that some thrust was being produced (Fig. 5A).

Vertical accelerations of both trunk markers and the COM reached a maximum during the downstroke and a minimum during the upstroke (Fig. 5). Vertical accelerations of trunk markers reached maximum and minimum values around the mid-downstroke and upstroke, respectively, whereas the vertical acceleration of the COM reached maximum and minimum values on the second half of the downstroke and upstroke, respectively (Fig. 5). Unlike horizontal accelerations, however, the offset between the timing of peak accelerations of the trunk markers and the COM did not seem to change as speed increased (Fig. 5).

These differences in timing and magnitude of accelerations of landmarks on the body and of the COM were reflected in the mean

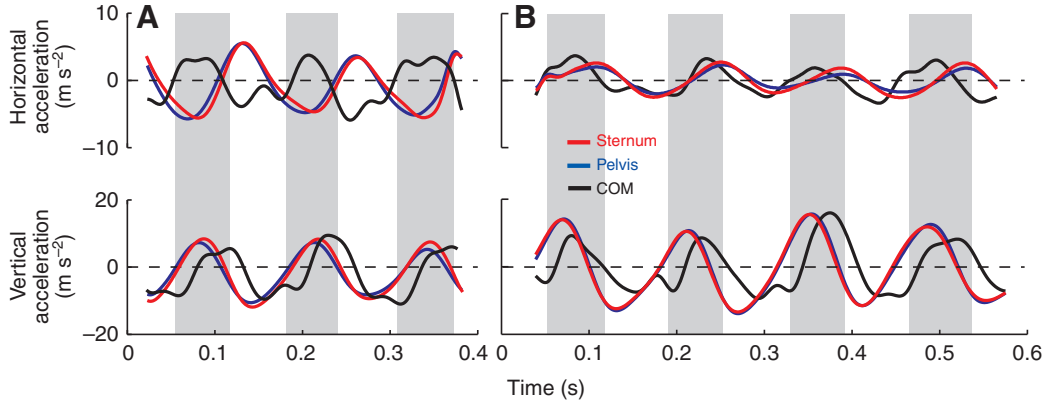

Fig. 5. Acceleration profiles over several wingbeat cycles at (A) 2.9 m s^{-1} and (B) 7.3 m s^{-1}, representing a slow and a fast flight for a representative *C. brachyotis* individual. Black lines correspond to accelerations of the COM, estimated from the mass model, and red and blue lines correspond to accelerations of the body-fixed sternum and pelvis markers, respectively. Vertical grey bars represent the downstroke portion of the wingbeat cycles.

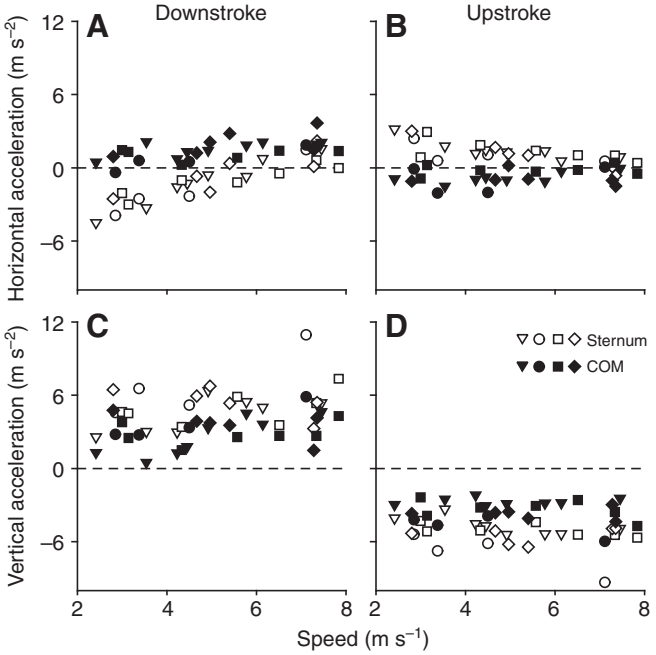

Fig. 6. Horizontal and vertical accelerations during downstroke and upstroke for the sternum marker (open symbols) and the COM (closed symbols). Each point corresponds to the mean value of all wingbeats (three to seven wingbeats) for a given trial. Different symbols represent the four *C. brachyotis* individuals used in this study.

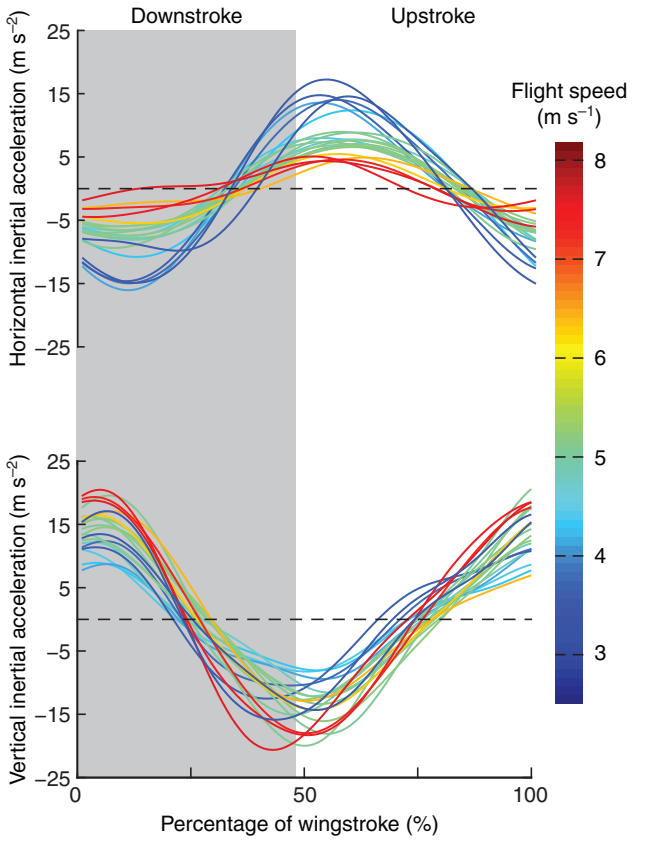

Fig. 7. Representative profiles of the horizontal and vertical components of the inertial accelerations over a standardized wingbeat of several trials for one *C. brachyotis* individual. Inertial accelerations were calculated as the difference between the accelerations calculated from an anatomical landmark (in this case, the sternum marker) and the accelerations of the estimated COM. The color of each line represents the flight speed for that particular trial and the vertical grey bar represents the downstroke portion of the wingbeat. Peaks values of the horizontal component of the inertial acceleration increases as flight speed decreases whereas peak values of the vertical component show no speed dependence.

accelerations at each speed. Had we inferred horizontal accelerations based on those of trunk markers alone, without accounting for inertial effects in any way, we would have arrived at the conclusion that, for the COM, negative horizontal acceleration was produced during downstroke and positive horizontal acceleration occurred during upstroke (Fig. 6A,B). However, our model, accounting for the time-varying distribution of the bat's mass during the wingbeat cycle, revealed the opposite: positive forward acceleration was produced during downstroke and negative acceleration during upstroke (Fig. 6A,B). Vertical accelerations of the body markers and the COM were similar, with positive mean accelerations during downstroke and negative mean accelerations during upstroke (Fig. 6C,D).

The difference between the acceleration of the markers and the acceleration of the estimated COM suggests that the inertial contribution to horizontal acceleration decreases with speed (Fig. 6A,B) whereas the contribution to vertical acceleration does not (Fig. 6C,D). Accordingly, when comparing the inertial acceleration throughout a wingbeat cycle, calculated as the difference between the accelerations of the body markers and the COM, bats showed large differences in horizontal peak inertial accelerations between low- and high-speed flights but peak values for vertical acceleration showed smaller differences among speeds (Fig. 7). To test the speed dependency of the inertial accelerations, we calculated the mean difference between the accelerations of the markers on the body and the acceleration of the estimated COM for both upstroke and downstroke. The difference between the contribution of the markers and the COM to horizontal accelerations decreased significantly in both downstroke and upstroke (GLM, speed effect: $F_{1,17}$=41.3, P<0.0001 and $F_{1,17}$=49.8, P<0.0001, respectively; see supplementary material Fig. S2). In contrast, the inertial contribution to vertical acceleration did not change with speed for either downstroke or upstroke (GLM, speed effect: $F_{1,17}$=1.90, P=0.19 and $F_{1,17}$=4.1, P=0.06, respectively; see supplementary material Fig. S2).

DISCUSSION

Our results support the idea that inertial accelerations produced by the flapping motion of relatively massive wings can considerably affect the kinematics of bat flight. We found substantial differences in timing and magnitude between accelerations of markers placed on the trunk and accelerations calculated from the estimated COM, in both horizontal and vertical accelerations.

Horizontal inertial effects were maximal in both peak and mean accelerations at slow speeds for the downstroke as well as for the upstroke phases of the wingbeat cycle and decreased as flight speed increased. One possible explanation for the decrease in horizontal inertial acceleration with speed is that the total horizontal excursion of the wing decreases with speed as a consequence of a more vertical stroke plane angle observed at higher speeds (see supplementary material Fig. S1). Thus, inertial effects can have important implications on the way we interpret horizontal accelerations, particularly during slow flights. In this study, if were we to base our analyses strictly on the movement of anatomical landmarks on the body, we would reach the

conclusion that during slow flight, *C. brachyotis* generates net thrust mostly during upstroke, supporting the idea that the tip-reversal upstroke is the principal generator of the thrust required. However, partitioning the movement of the flying animal into specific motions of the COM and the specific motion of the other regions of the 'distributed mass', particularly the wings, relative to the COM, changes the picture substantially. Our results show that, contrary to the common view of slow flight in bats, *C. brachyotis* do not generate enough thrust to produce a forward acceleration of the COM during the upstroke at low speeds where the backward flick of the wingtip occurs. We conclude, therefore, that horizontal accelerations calculated from the motion of landmarks on the body alone, without controlling for inertial effects due to the flapping motion of the wings, would have led to the incorrect conclusion that net thrust is produced during the upstroke at the analyzed low speeds. Positive horizontal acceleration of the COM occurs almost exclusively during the downstroke whereas net negative horizontal accelerations are experienced during the upstroke at the studied speeds. It is possible that, as flight speed decreases, upstroke thrust would become more important and that net thrust could be found. Unfortunately, we could not train our bats to fly at slower speeds in the wind tunnel. However, as our data suggest, the proportion of marker accelerations that are caused by the inertial effects of the wing motion would also increase, making the estimation of the aerodynamic forces produced during slow flight prone to error unless analyses accurately consider the effect of the wing masses and their accelerations. It is worth noting that the absence of net thrust does not necessarily imply that no thrust is being generated during the upstroke. Similarly to what has been documented in one bat species (Hedenström et al., 2007; Johansson et al., 2008), it could be the case that our bats generate some thrust during upstroke, and although this thrust not enough to overcome drag, it might be important for stable and/or energetically efficient flight. However, without an estimation of drag it is very difficult to assess the relative importance of the generated thrust.

In contrast to horizontal aerodynamic forces, our understanding of the relative timings of net vertical aerodynamic forces was not influenced by the mass model. During the downstroke, the inertial effects of the wings moved the trunk markers upwards, and during the upstroke, the opposite motion of the wing translated the trunk markers downwards (Fig. 1B). The net result is that the motions of body markers exaggerated the apparent magnitude of the bat's vertical accelerations compared with the vertical acceleration of the COM (Fig. 1B). Mean vertical acceleration of the COM during upstroke fluctuated between –3 and –6 $m\,s^{-2}$ at all speeds (Fig. 6D) instead of the –9.8 $m\,s^{-2}$ expected during an aerodynamically inactive upstroke. This could potentially be explained by the mismatch between the timing of vertical acceleration and the wingbeat phases. As can be observed during slow flight (Fig. 5A), vertical acceleration becomes positive around mid-downstroke and continues through the beginning of the upstroke. This would result in a diminished mean vertical acceleration for both downstroke and upstroke. If one employed the excursions of the wingtip to define the upstroke and downstroke phases of the wingbeat cycle, instead of the movement of the wrist (as in this study), mean vertical accelerations during upstroke would likely be closer to the gravitational constant. Alternatively, *C. brachyotis* may generate some lift during upstroke as well as during downstroke. Direct experimental support for this hypothesis comes from PIV studies that have shown partially active upstrokes in *C. brachyotis* flying at both slow (Tian et al., 2006) and intermediate speeds (Hubel et al., 2009; Hubel et al., 2010). We also observed a reduction in downward acceleration of the COM during the second half the upstroke at both low and high speeds (Fig. 5), which provides additional evidence in support of the idea of lift generation during at least a portion of the upstroke.

Previous work has considered the possibility that inertial forces produced by the motion of the wings could influence the dynamics of bat flight, but concluded that net thrust occurs during tip-reversal upstrokes (Aldridge, 1987). In that study of six bat species, inertial acceleration produced by wing motion was computed from an estimation of the angular acceleration of the wingtip and the assumption that the wing can be well represented as fully extended during the wingbeat. However, during both the downstroke and upstroke portions of the wingbeat cycle, the wings present a three-dimensionally complex geometry that differs substantially from a completely extended wing (Swartz et al., 2005). Wing form differs even more from the extended form during the upstroke than the downstroke, where the wings fold in a complex fashion and are brought close to the body by significant flexion of the elbow and wrist (Aldridge, 1986; Lindhe Norberg and Winter, 2006; Norberg, 1976; Riskin et al., 2008; Tian et al., 2006; Wolf et al., 2010). As a consequence, estimates of inertial accelerations produced by the motion of the wing with respect to the body that are based on the angular acceleration of the extended wing are likely unreliable. To adequately assess upstroke function, a more detailed model that combines accurate kinematics and accounting of the three-dimensional distribution of wing mass, such as we have provided here, is required. We predict that when inertial effect are accounted for in studies of other bats, in a matter analogous to the methods we used in this study, estimations of accelerations of the COM of bats in a broad range of species will show substantial differences to accelerations measured from anatomical landmarks on the trunk.

One challenge to the accuracy of our model is associated with the determination of the mass distribution of the head, thorax and abdomen. We estimated the body's mass as uniformly distributed throughout an ellipsoid, the position of which was based on the position of the pelvis, sternum and shoulder markers; a more realistic anatomical model could account for the variations in density within these structures that comprise very dense bone, tissues of moderate density such as muscle, and regions of low density such as lungs and tracheal and pharyngeal spaces. Because the horizontal excursions of the wing are far smaller than its vertical excursions, errors in body mass distribution estimates will have a relatively larger effect on the estimated horizontal position of the COM. Thus, pitching motions of the body might have an important effect on the estimation of horizontal accelerations. To explore the effect of this assumption, we compared this model with one in which we estimated the body mass as a point mass located between the sternum and the pelvis markers. This alternative model did not significantly change the results presented here (data not shown). Thus, although there is potential for error in the estimations of horizontal accelerations, our data are consistent with the hypothesis that no mean net thrust is present during upstroke at the range of speeds we measured.

We conclude that accelerations computed from landmarks placed on the trunk do not accurately represent the accelerations of the COM throughout the wingbeat cycle, and that the differences are likely due to the inertial effect produced by the flapping of the relatively massive wings. We suggest that this has implications for the analysis of the kinematics and dynamics of not only bat flight, but also that of other vertebrate flyers, as evidenced by the substantial effect of wing motion on the flight kinematics of

cockatiels (Hedrick et al., 2004). These results highlight the importance of the incorporation of inertial effects in future analyses of the kinematics of flapping locomotion in order to ascertain the magnitude of these effects among flight behaviors and among species, and determine how they vary with factors such as flight speed and body size.

ACKNOWLEDGEMENTS

All experiments were conducted at the Concord Field Station (CFS) at Harvard University, and we express our thanks to the CFS staff, especially A. A. Biewener for allowing us the use of the facilities, and P. Ramírez for taking care of the bats. Bats were provided through the generous support of Dr Allyson Walsh and the Lubee Bat Conservancy. We also thank members of the Swartz and Breuer laboratory groups at Brown University for the help provided during the experiments and during the analysis of data. This manuscript was greatly improved by conversations with T. Y. Hubel, the Morphology Group at Brown University and the comments of anonymous reviewers. This work was supported by the Air Force Office of Scientific Research (AFOSR), the NSF-ITR program and the Bushnell Foundation.

REFERENCES

Abdel-Aziz, Y. I. and Karara, H. M. (1971). Direct linear transformation from comparator coordinates into object space coordinates in close-range photogrammetry. In *Proceedings of the Symposium on Close-Range Photogrammetry*, pp. 1-18. Falls Church, VA: American Society of Photogrammetry.

Aldridge, H. D. J. N. (1986). Kinematics and aerodynamics of the greater horseshoe bat, *Rhinolophus ferrumequinum*, in horizontal flight at various speeds. *J. Exp. Biol.* **126**, 479-497.

Aldridge, H. D. J. N. (1987). Body accelerations during the wingbeat in six bat species: the function of the upstroke in thrust generation. *J. Exp. Biol.* **130**, 275-293.

Aldridge, H. D. J. N. (1991). Vertical flight in the greater horseshoe bat *Rhinolophus Ferrumequinum*. *J. Exp. Biol.* **157**, 183-204.

Alexander, D. A. (2002). *Nature's Flyers: Birds, Insects, and the Biomechanics of Flight*. Baltimore: The Johns Hopkins University Press.

Azuma, A. (2006). *The Biokinetics of Flying and Swimming*. Reston. VA: American Institute of Aeronautics and Astronautics.

Barlow, J. B., Rae, W. H. and Pope, A. (1999). *Low-Speed Wind Tunnel Testing*. New York: Wiley.

Bilo, D., Lauck, A. and Nachtigall, W. (1984). Measurement of linear body accelerations and calculation of the instantaneous aerodynamic lift and thrust in a pigeon flying in a wind tunnel. In *Biona-Report*, Vol. 3 (ed. W. Nachtigall), pp. 87-108. Stuttgart: Gustav Fischer.

Brown, R. H. J. (1948). The flight of birds: the flapping cycle of the pigeon. *J. Exp. Biol.* **25**, 322-333.

Brown, R. H. J. (1953). The flight of birds. II. Wing function in relation to flight speed. *J. Exp. Biol.* **30**, 90-103.

Hedenström, A., Johansson, L. C., Wolf, M., von Busse, R., Winter, Y. and Spedding, G. R. (2007). Bat flight generates complex aerodynamic tracks. *Science* **316**, 894-897.

Hedenström, A., Muijres, F., von Busse, R., Johansson, L., Winter, Y. and Spedding, G. (2009). High-speed stereo DPIV measurement of wakes of two bat species flying freely in a wind tunnel. *Exp. Fluids* **46**, 923-932.

Hedrick, T. L. (2008). Software techniques for two- and three-dimensional kinematic measurements of biological and biomimetic systems. *Bioinspir. Biomim.* **3**, 034001.

Hedrick, T. L., Tobalske, B. W. and Biewener, A. A. (2002). Estimates of circulation and gait change based on a three-dimensional kinematic analysis of flight in cockatiels (*Nymphicus hollandicus*) and ringed turtle-doves (*Streptopelia risotia*). *J. Exp. Biol.* **205**, 1389-1409.

Hedrick, T. L., Usherwood, J. R. and Biewener, A. A. (2004). Wing inertia and whole-body acceleration: an analysis of instantaneous aerodynamic force production in cockatiels (*Nycphicus hollandicus*) flying across a range of speeds. *J. Exp. Biol.* **207**, 1689-1702.

Hubel, T. Y., Hristov, N. I., Swartz, S. M. and Breuer, K. S. (2009). Time-resolved wake structure and kinematics of bat flight. *Exp. Fluids* **46**, 933-943.

Hubel, T. Y., Riskin, D. K., Swartz, S. M. and Breuer, K. S. (2010). Wake structure and wing kinematics: the flight of the lesser dog-faced fruit bat, *Cynopterus brachyotis*. *J. Exp. Biol.* **213**, 3427-3440.

Johansson, L. C., Wolf, M., von Busse, R., Winter, Y., Spedding, G. R. and Hedenstrom, A. (2008). The near and far wake of Pallas' long tongued bat (*Glossophaga soricina*). *J. Exp. Biol.* **211**, 2909-2918.

Lindhe Norberg, U. M. and Winter, Y. (2006). Wing beat kinematics of a nectar-feeding bat, *Glossophaga soricina*, flying at different flight speeds and Strouhal numbers. *J. Exp. Biol.* **209**, 3887-3897.

Norberg, U. M. (1976). Aerodynamics, kinematics, and energetics of horizontal flapping flight in the long-eared bat *Plecotus auritus*. *J. Exp. Biol.* **65**, 179-212.

Norberg, U. M. (1990). *Vertebrate Flight*. Berlin: Springer-Verlag.

Riskin, D. K., Willis, D. J., Iriarte-Díaz, J., Hedrick, T. L., Kostandov, M., Chen, J., Laidlaw, D. H., Breuer, K. S. and Swartz, S. M. (2008). Quantifying the complexity of bat wing kinematics. *J. Theor. Biol.* **254**, 604-615.

Riskin, D. K., Iriarte-Díaz, J., Middleton, K. M., Breuer, K. S. and Swartz, S. M. (2010). The effect of body size on the wing movements of pteropodid bats, with insights into thrust and lift production. *J. Exp. Biol.* **213**, 4110-4122.

Swartz, S. M. (1997). Allometric patterning in the limb skeleton of bats: implications for the mechanics and energetics of powered flight. *J. Morphol.* **234**, 277-294.

Swartz, S. M., Groves, M. D., Kim, H. D. and Walsh, W. R. (1996). Mechanical properties of bat wing membrane skin. *J. Zool.* **239**, 357-378.

Swartz, S. M., Bishop, K. L. and Ismael-Aguirre, M.-F. (2005). Dynamic complexity of wing form in bats: implications for flight performance. In *Functional and Evolutionary Ecology of Bats* (ed. Z. Akbar, G. McCracken and T. H. Kunz), pp. 110-130. Oxford: Oxford University Press.

Thollesson, M. and Norberg, U. M. (1991). Moments of inertia of bat wings and body. *J. Exp. Biol.* **158**, 19-35.

Thomas, A. L. R., Jones, G., Rayner, J. M. V. and Hughes, P. M. (1990). Intermittent gliding flight in the pipistrelle bat (*Pipistrellus pipistrelus*) (Chiroptera: Vespertilionidae). *J. Exp. Biol.* **149**, 407-416.

Tian, X., Iriarte-Diaz, J., Middleton, K., Galvao, R., Israeli, E., Roemer, A., Sullivan, A., Song, A., Swartz, S. and Breuer, K. (2006). Direct measurements of the kinematics and dynamics of bat flight. *Bioinspir. Biomim.* **1**, S10-S18.

Tobalske, B. W. (2007). Biomechanics of bird flight. *J. Exp. Biol.* **210**, 3135-3146.

Watts, P., Mitchell, E. J. and Swartz, S. M. (2001). A computational model for estimating the mechanics of horizontal flapping flight in bats: model description and validation. *J. Exp. Biol.* **204**, 2873-2898.

Wolf, M., Johansson, L. C., von Busse, R., Winter, Y. and Hedenstrom, A. (2010). Kinematics of flight and the relationship to the vortex wake of a Pallas' long tongued bat (*Glossophaga soricina*). *J. Exp. Biol.* **213**, 2142-2153.

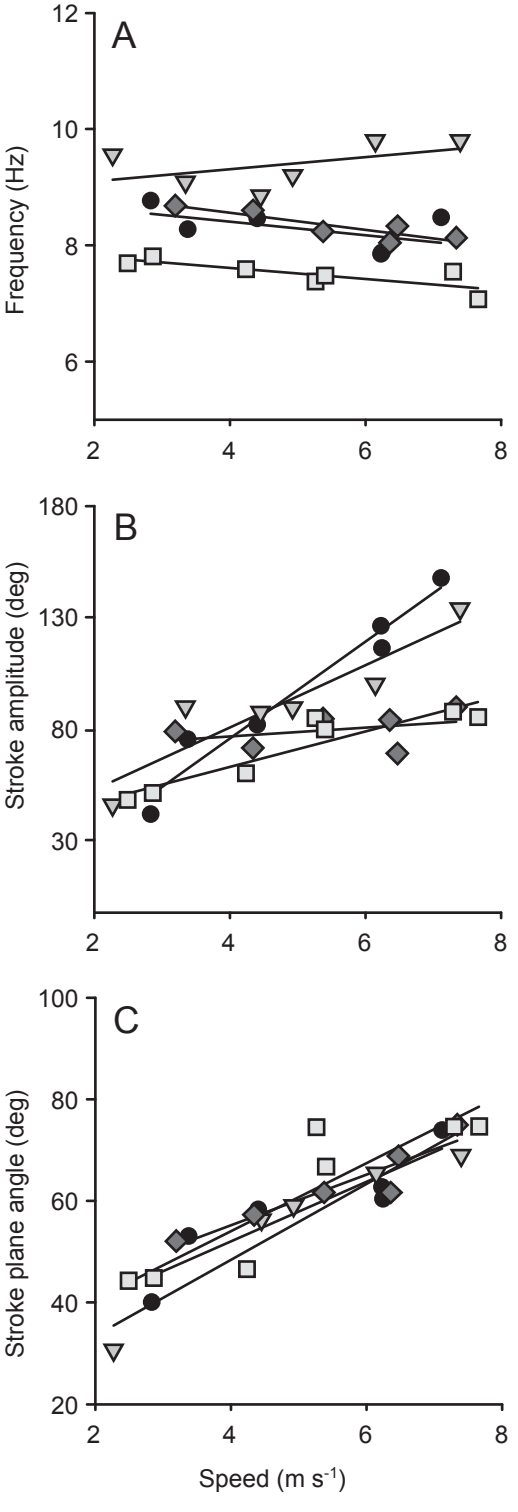
A
Frequency (Hz)
12
10
8
6
2
4
6
8
B
Stroke amplitude (deg)
180
130
80
30
2
4
6
8
C
Stroke plane angle (deg)
100
80
60
40
20
2
4
6
8
Speed (m s-1)

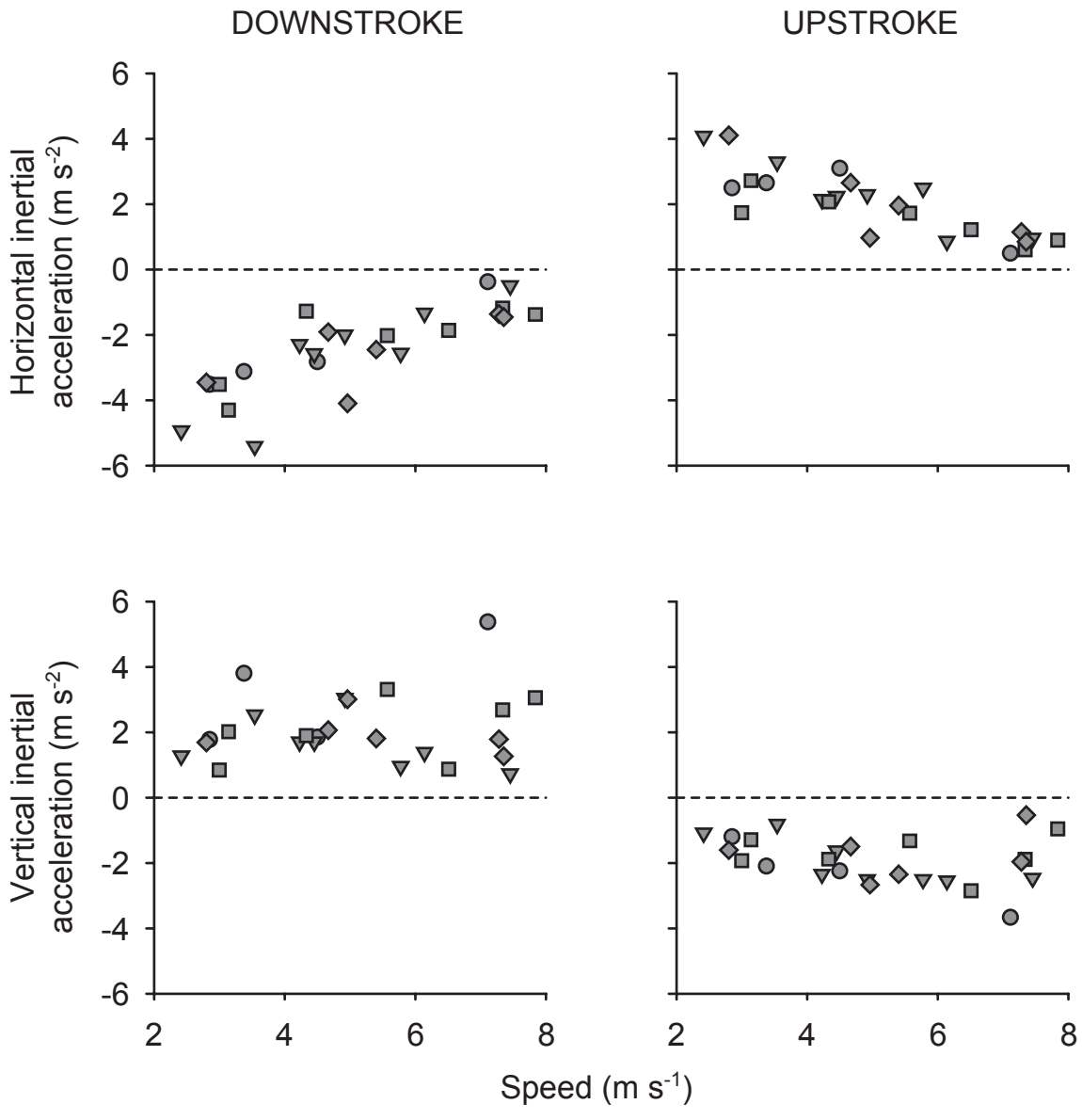
DOWNSTROKE
UPSTROKE
Horizontal inertial acceleration (m s-2)
Vertical inertial acceleration (m s-2)
6
4
2
0
-2
-4
-6
2
4
6
8
Speed (m s-1)